Applied Surface Science 455 (2018) 780–788

Contents lists available at ScienceDirect

Applied Surface Science

journal homepage: www.elsevier.com/locate/apsusc

Full Length Article

Incorporation of silver nanoparticles on Ti7.5Mo alloy surface containing TiO_2 nanotubes arrays for promoting antibacterial coating – In vitro and in vivo study

Ana Paula Rosifini Alves Claro[a,*], Reginaldo T. Konatu[a], Ana Lúcia do Amaral Escada[a], Miriam Celi de Souza Nunes[b], Cláudia Vianna Maurer-Morelli[b], Marcela Ferreira Dias-Netipanyj[c], Ketul C. Popat[c], Diego Mantovani[d]

[a] UNESP–São Paulo State University, School of Engineering, Materials and Technology Department, Guaratinguetá, SP, Brazil
[b] UNICAMP – University of Campinas, Faculty of Medical Sciences, Department of Medical Genetics, Campinas, São Paulo, Brazil
[c] Colorado State University, Department of Mechanical Engineering/School of Biomedical Engineering, Fort Collins, CO, USA
[d] Laval University, Metallurgy and Materials Engineering, Department of Mining, Québec City, Quebec, Canada

ARTICLE INFO

Keywords:
Nanotubes
Titanium alloys
Antibacterial activity
Silver nanoparticles

ABSTRACT

Bulk and surface properties are very important for materials used in biomedical applications. The development of new surface treatments, such as antibacterial coatings can directly affect the response of the surface. The purpose of this study was the development of antibacterial coating on the Ti7.5Mo alloy surface combining TiO_2 nanotubes with silver nanoparticles incorporation using polydopamine assisted immobilization technique. Surface characterization analysis showed that silver nanoparticles were successfully immobilized. The concentration established was bactericidal, i.e., no bacteria grew after incubation. In vivo results showed that silver incorporation on the surface containing TiO_2 nanotubes did not cause altered locomotor activity in zebrafish. On the other hand, it affected the cell adhesion on the surface. Thus, these results confirm the hypothesis that silver nanoparticles were totally incorporated to polydopamine on the surface containing TiO_2 nanotubes and acted as the main mechanism the death of the bacteria by contact.

1. Introduction

The major challenge in the development of materials for biomedical applications is to obtain a material with excellent bulk and surface properties. When a biomaterial is inserted into human body it must exhibit a good interaction with the tissue with favorable response. The surface properties such as chemical composition, surface energy and topography are essential for success of implant and favorable host response. However, several studies have shown that bacterial infections on biomaterial is a major problem that may lead to failure of the implant.

Surface roughness is beneficial for osseointegration and bone anchorage for orthopedic implants [1–4]; however, it may induce bacterial adhesion on the implant surface. Adhered bacteria may form biofilm that acts as a medium for supplying nutrients to the bacteria inside the dense biofilm [5,6]. Recent studies related to modifying surface topography showed it improved the cellular adhesion and some instances reduce bacterial adhesion [7] compare to techniques using antibacterial nanoparticles incorporation on the surface [8–10].

Antimicrobial agents can be incorporated on the surface of a biomaterial using polymeric coatings. Mussel inspired polydopamine (PDA) was found to produce thin films coating with several functional uses. Catechol and amino groups are present in PDA and exhibit metal binding ability. They could combine strongly with various metal ions, such as silver and copper, by chelation, through dip-coating in silver nitrate or chloride solutions, respectively (haeshin). The production of antibacterial coating using a polydopamine film for metal ions immobilization have been studied by Saidin et al. [11]. The functionalization of the stainless steel surface through a multi-step process of dopamine polymerization, Ag metallization and HA biomineralization was evaluated. The SS316L substrates were first pre-treated and grafted with polydopamine through a self-polymerization technique. The Ag nanoparticles were then metallized on the polydopamine film, followed by the formation of second layer polydopamine film. HA biomineralization was performed in 1.5 Simulated Body Fluid (SBF) solution. The antibacterial activity of the coating was investigated on Escherichia

* Corresponding author.
E-mail address: rosifini@feg.unesp.br (A.P.R. Alves Claro).

https://doi.org/10.1016/j.apsusc.2018.05.189
Received 12 December 2017; Received in revised form 19 May 2018; Accepted 24 May 2018
Available online 31 May 2018
0169-4332/

coli (E. coli) and concluded that the antibacterial effect was dependent on the Ag composition. The introduction of low amount of Ag (metallization at 12 h) has partly killed the cells while highest Ag percentage (metallization at 24 h) has killed the E. coli colonies with 97.88% bactericidal ratio. Moreover, the metallization at 24 h not retarded the biomineralized HA. In this case, the bacteria were killed by an electrostatic interaction between the positive charge of Ag and the negative charge of bacterial membrane has led to the formation of pit on the membrane. It has increased the membrane permeability, diffusion of Ag + ions into the cells and diffusion of the intracellular matrix outside of the cell, further causing the cell was shrunk and dead. However, this approach has not been investigated with titanium and its alloys.

Jia et al. [12], demonstrated a simple, controllable and cost-effective approach to produce biomimetic hierarchical TiO_2/Ag coatings by combining the MAO technique with mussel-inspired metallization. They studied the antibacterial power of this surface and observed that *S. aureus* were killed by the so-called "trap-killing" principle, which might include: down-falling and collision with pore walls; nanosilver binding via electrostatic attraction or specific interactions such as Ag-thiol bond and membrane distortion and destruction by nanosilver and local Ag for one or more bacteria. This surface treatment did not alter the cellular functions of osteoblast-like MG-63 in vitro nor serious inflammatory response in a rabbit model in vivo.

In the present study, we combine the surface of the alloy Ti7.5Mo containing TiO_2 nanotubes obtained by anodic oxidation based in our previous researches [13–15] with PDA to immobilize silver nanoparticles to form antibacterial surfaces. To assess the biological performances of these coatings, bacterial growth was evaluated using biofilms and cell function was investigated by cell adhesion and proliferation.

2. Experimental procedure

Ti7.5Mo alloy was prepared using arc melting furnace with water-cooled copper crucible and high purity argon atmosphere from Ti (99.9%) and Mo (99.8%) sheet as raw materials. The ingots were re-melted for 10 times and flipped over after each melting to ensure chemical homogeneity due to differences between melting point of elements. They were homogenized at 1000 °C for 24 h and cooled inside the tubular furnace. The homogenized ingots were cold rolled in rotary swaging at room temperature (final diameter about 10 mm), solution treated at 950 °C for 2 h and quenched into water.

From the bars, 3 mm-thick discs were obtained and they were used as substrates for the growth of TiO_2 nanotubes. Before anodic oxidation, they were polished using silicon carbide (SiC) paper (#100–#1200 grit), polished with clothes using silica colloidal (OPS- Struers) plus 5% oxalic acid and cleaned in ultrasonic bath in water (20 min), in alcohol (20 min) and in acetone (20 min).

Polished samples were used as a working electrode in anodization setup. The process was performed according our previous anodization studies for Ti7.5Mo alloy [13–15] using 20 V for, 24 h in electrolyte composed of water/glycerol containing 0.25 wt% NH_4F. Platinum was used as counter electrode. After anodization, samples were rinsed in distilled water and dried in oven. The as-anodized samples were annealed at 450 °C for 1 h for the phase transformation and left to cool inside the oven at 40 °C.

For antibacterial coating with silver, samples were immersed in dopamine solution (2g/L) at room temperature for 24 h. Solution was prepared by dissolving dopamine in a Trizma® (Tris base) solution (10 mM, pH 8.6) with stirring until all the crystals were dissolved. The pH was corrected by the addition of some drops of HCl so that final pH was 8.5. After the polymerization samples were rinsed with DI water to remove the excess of dopamine from the surface. Fresh coated samples were immersed in a silver nitrate solution (50 mM) at room temperature in dark for 18 h. After this time, samples were rinsed with DI water and dried.

2.1. Surface characterization

The surface morphology and chemistry were investigated by field emission scanning electron microscopy (FEG-SEM; Magellan 400, FEI) equipped with energy dispersive X-ray spectroscopy (EDS). The phases formed were evaluated by X-Rays diffraction (XRD) using a PANanalytical Empyrean diffractometer operated at an accelerating voltage of 40 kV, a current of 25 mA, scanning speed of 0.02°/min with Cu Kα radiation.

X-Rays photoelectron spectroscopy (XPS, PHI 5600-ci Spectrometer, Physical Electronics, Eden Prairie, MN, USA) under aluminum (1486.6 eV) and magnesium irradiation (1253.6 eV) was used to evaluate chemical composition of the samples. The direction of the photoelectron detection angle was 45° and a surface area of the 0.05 cm^2 was used to obtain broad spectra.

Contact angle measurements were obtained using the sessile drop method with a contact angle goniometer (Kruss DSA 100S). A water drop of 10 μL was added and the average of three readings on three samples of each group was used.

2.2. In vitro studies

2.2.1. Bacterial analysis

Two reference strains [American Type Culture Collection (ATCC), *Candida albicans* (ATCC 18804) and *Streptococcus mutans* (ATCC 35688)] were used in this study. Standard suspensions of each strain with optical densities equivalent to 10^6 cells/mL were prepared. For this purpose, the strains were seeded in Sabouraud agar (Difco, Detroit, USA) for *C. albicans* or brain heart infusion (BHI) agar (Difco, Detroit, USA) for *S. mutans* and incubated at 37 °C for 24 h.

After incubation, the cells were resuspended in sterile saline solution [0.9% sodium chloride (NaCl)], and the number of cells in the suspension was counted in a spectrophotometer (B582, Micronal, São Paulo, Brazil). The optical density and wavelength parameters used were 0.284 and 530 nm for *C. albicans*; and 0.620 and 398 nm for *S. mutans*.

The biofilms were grown on 30 discs (10 mm of diameter and 3 mm of thickness). The discs were placed in the first rows of 24-well plates (Costar Corning, New York, USA) containing 2 mL of sterile brain heart infusion (BHI) broth (Difco, Detroit, USA) supplemented with 5% sucrose and inoculated with 0.1 mL of each microbial suspension. The discs were then incubated at 37 °C for 48 h. The media was not changed during the incubation period. All incubations were performed at a partial pressure of 5% CO_2.

After 48 h of incubation, the discs containing the biofilms were aseptically transferred to the second and third rows of the plate (24 wells) and washed twice with 2 mL of 0.9% NaCl to remove loosely bound material.

The discs were placed in tubes containing 10 mL of 0.9% NaCl and sonicated (Sonoplus HD 2200, 50 W Bandelin Eletronic, Berlin, Germany) for 30 s to disperse the biofilms. Biofilms suspensions were serially diluted in 0.9% NaCl to give dilutions of 10^{-1}–10^{-5} times the original concentration. One hundred microliter aliquots of each dilution were seeded on agar (in duplicate): Sabouraud dextrose agar with 50 mg/L chloramphenicol (União Química, São Paulo, Brazil) for *C. albicans*, and Mitis Salivarius agar (Difco, Detroit, USA) supplemented with 0.2 IU/mL bacitracin (União Química, São Paulo, Brazil) and 15% sucrose to *S. mutans*. After 48 h of incubation, the number of colony-forming units per milliliter (CFU/mL) was determined. The results were

log-transformed (log_{10}) and analyzed by analysis of variance (ANOVA) and the Tukey test. A P value < 0.05 was considered to indicate a statistically significant difference.

2.2.2. Cell culture

Adipose Derived Stem Cells (ADSCs) were donated by Dr. Kimberly Cox-York from the Department of Food Science and Human Nutrition, Colorado State University. ADSCs were cultured at 37 °C and 5% CO_2 in growth media consisting of MEM-Alpha Modification Media, GE Life Science-Hyclone with 10% of Fetal Bovine Serum (FBS) and 1% of penicillin/streptomycin (Sigma). The growth media was changed every other day. To the tests on surfaces the cells were detached using 0.25% Trypsin-EDTA, centrifuged at 1000 rpm for 10 min. Following centrifugation, the cells were counted at concentration of 5×10^3, using Neubauer chamber and Trypan Blue. Cells were seeded on all surfaces in 24 well plates.

The activity of lactate dehydrogenase (LDH) in the culture media release by the cell was used as an index of cytotoxicity. After incubation for 1 day, the culture media were sampled and centrifuged, and the supernatant was used for the LDH activity assay

The cell viability was measured after 1 and 7 days of culture using Alamar Blue Assay Reagent (Promega). Adhered cells were incubated at 37 °C for 4 h in fresh α-MEM and 10% of Alamar Blue Reagent. The Alamar Blue Reagent is an oxidized form redox indicator that is blue in color. When incubated with viable cells, the reagent changes color from blue to red. After 4 h the optical density (OD) of solution was measured at 570 and 600 nm using a spectrophotometer (FLU Ostar Omega; BMG Labtech, Durham, NC). The percentage reduction of Alamar Blue was calculated as described by the company instructions (Thermo-scientific).

After 1 and 7 days of initial culture the cell adhesion and proliferation were investigated by fluorescence staining with Rhodamine Phalloidin (Cytoskeleton, Inc.) at 70 nM, and 4′ 6-diamidino-2-phenylindole DAPI (Life Technologies) at 300 nM. The surfaces were removed from the growing media, washed with PBS and fixed with 3.7% of formaldehyde for 15 min at room temperature. To permeabilize the cells, the surfaces were incubated with 1% of Triton-X100 for 3 min, and then washed with PBS. The surfaces were incubated in rhodamine-phalloidin stain at a concentration of 70 nM for 30 min at room temperature. After 25 min of rhodamine-phalloidin staining, DAPI was add at concentration of 300 nM for 5 min. All the solution was aspirated, and the surfaces were then washed with PBS and imaged using a Zeiss Axioplan 2 fluorescence microscope. The number of adhered cells on the surfaces was determined from 10X DAPI stained images by counting the nuclei. These analyses were performed using “Analyze Particles” feature embedded in the ImageJ software. The cell area was measured from 10× rhodamine-phalloidin stain by analysis of cytoskeleton-actin filaments, the analysis was conducted using pixels of “Masks” in the ImageJ software.

The morphology of ADSCs adhered on the surfaces were evaluated using Scanning Electron Microscopy (SEM) after 1 and 7 days of culture. SEM was done to visualize how cells interacted with the surfaces. The cells were fixed in a solution of 3% glutaraldehyde (Ted Pella), 0.1 M sodium cacodylate (Alfa Aesar), and 0.1 M sucrose (Fisher Scientific) for 45 min. The surfaces were then incubated in buffer solution of 0.1 M sodium cacodylate (Alfa Aesar) and 0.1 M sucrose (Fisher Scientific) for 10 min. After fixation, the cells were dehydrated in increasing concentration of ethanol (35%, 50%, 70% and 100%) for 10 min each. Further, the surfaces were dehydrated by incubating in hexamethyldisilane (HMDS, Sigma) for 10 min. The surfaces were coated with 10 nm of gold and stored in a desiccator until analysis using SEM.

All the quantitative results were analyzed using mean ± SD and $n_{min} = 5$. Statistical significance was considered at (*) $p < 0.05$, (**) $p < 0.01$ and (***) $p < 0.001$ using one-way ANOVA test and Tukey HSD to multiple comparisons, SPSS 13.0 windows software.

2.3. In vivo study – Zebrafish animal model

In this study, we used Zebrafish animal model to perform the behavioral analysis. The Zebrafish *(Danio rerio)* is a tropical freshwater fish used in the fields of toxicology and biomedical research. It has been widely used due to characteristics such as small size making manipulation relatively easy, very high reproducibility, quick development and transparency of the embryo [16,17]. All zebrafish experiments were approved by the Ethical Committee for Animal Research, University of Campinas, CEUA #4444-1.

Wild-type zebrafish were maintained in a temperature-controlled room at 26 ± 2 °C and with a 14 h light/10 h dark cycle. Animals were kept in 30–50 L tanks (two animals per liter) filled with non-chlorinated water cleared with mechanical and chemical filtration. Adults fish were fed three times/day with commercial flake fish food (Tetramin, Tetra, Blacksburg, VA, USA) and artemia supplementation, once a day. Eggs were collected after natural spawning in a Petri dish and viable fertilized eggs were selected under a Stereomaster Digital Zoom Microscope (Fisher Scientific).

For studies, fertilized eggs were transferred to plates with 24-wells along with 1.9 mL of solution and incubated for 120 h in an incubator at 28.5 °C and 14 h light/10 h dark cycle. Each solution was prepared from samples according to protocol stablished for us and as describe bellow. The same groups evaluated in the cell culture were evaluated in zebrafish larvae: TiO_2 nanotubes (TNT) and TNT/PDA/Ag, being the latest divided into three subgroups according to immersion time, Day 1, Day 4 and Day 7, respectively. For each concentration, three replicates were evaluated, which resulted in 30 embryos exposed to each concentration. Aquarium water was used as control group. After 5 days of exposition, according to their groups, larvae were transferred to a Petri dish filled with aquarium water and fed with paramecia.

At 5 and 7 days post fertilization larvae were distributed in a 96-well plate (n = 15 each group) in a semi-randomized way for locomotor activity assay using an automated computerized video-tracking system DanioVision (Noldus, Wageningen, The Netherlands). Distance and speed were recorded for each larva in both ages using the EthoVision XT locomotion tracking software (Noldus, Wageningen, The Netherlands). The non-parametric Kruskal-Wallis test followed by Dunn’s post hoc test was performed to determine statically significant differences between groups using GraphPad Prism version 7.0 (GraphPad Software, San Diego, CA, USA). Data are presented as mean values ± SEM and the significance level were set at $p \leq 0.05$.

The determination of the silver concentration released during tests for each group was measured using anodic stripping voltammetry (ASV). This technique has been used for measured of trace amounts of silver ions release in aqueous solutions [18–20]. A scan voltammetry with a glassy carbon electrode as a working electrode, Pt electrode as auxiliary electrode and Ag/AgCl electrode as a reference electrode was used to measure the released Ag_0 concentration after samples immersion during 1, 4 and 7 days. A blank solution of KNO_3 and HSO_4 (0.1 M) was stirring in accumulation potential of (E) – 0.7 V for 800 s. Scan voltammetry was proceeded from 0.0 to 0.75 V, a scan rate of 100 mV s^{-1}, a background spectrum was obtained using an Autolab PGSTAT-30 potentiostat. For each analysis was prepared a new blank solution and measured the background.

3. Results and discussion

3.1. Surface characterization

After anodization, highly ordered and vertically oriented nanotubes were formed on Ti7.5Mo alloy surface as shown in Fig. 1. The average diameter was approximately 57 nm and wall thickness 19 nm, well-aligned nanotubes of 1220 μm in length (inset of Fig. 1b); thus value is consistent with our previous studies with this alloy with good results [14,15,21].

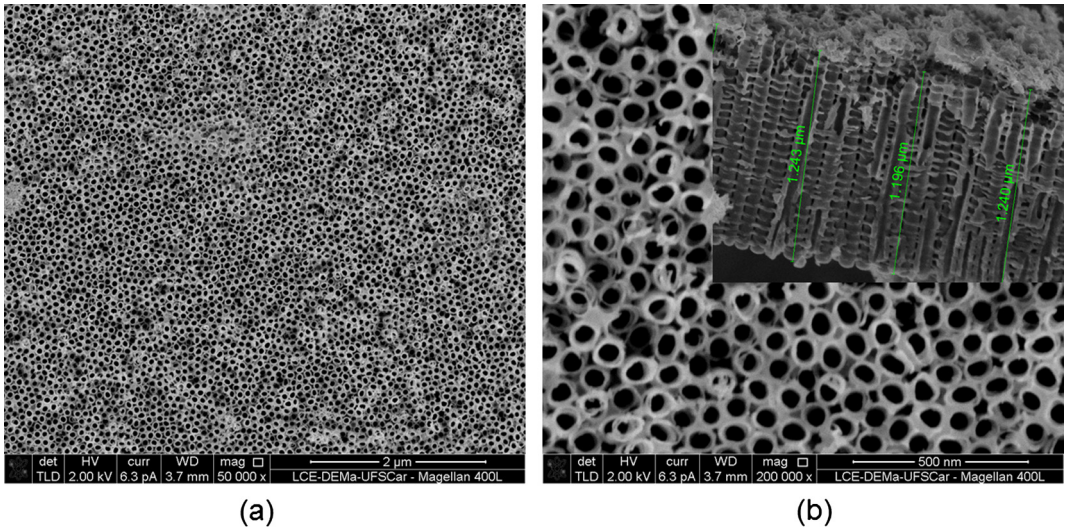

Fig. 1. Representative micrographs of the TiO_2 nanotubes on Ti7.5Mo alloy surfaces. Top view SEM images (a) low and (b) high magnification. The insets show the cross section magnified images of the length of TiO_2 nanotubes.

In Fig. 2 is possible to see the top surface of the Ti7.5Mo alloy after PDA grafted and immersion in $AgNO_3$. It can be observed that dopamine coating did not modify the appearance of the surface containing TiO_2 nanotubes since no changes in morphology was observed. After coating, nanoparticles appeared on the surface indicating the deposition of silver nanoparticles confirmed by EDS analysis (Fig. 2b).

X-Ray diffraction was used to evaluate the phase composition and crystal structure of the samples for each step (Fig. 3). The XRD pattern show peaks of anatase phase after anodic oxidation (Ti7.5Mo + TNT samples). In addition, Ag peaks were detected for samples after coating with polydopamine and silver (Ti7.5Mo + TNT + PDA + Ag samples). These results can be attributed to the incorporation of silver by the nanotubes, it being evident in SEM images that only a few silver particles are found in the surface. Studies have shown the silver detection on the surface with silver concentration and verified an increase of the intensity of peaks according to the increase of the employed concentrations [22–24].

XPS analysis was done to confirm the Ag incorporation in TiO_2 nanotubes. Fig. 4 shows the XPS wide scan of the samples after anodic oxidation (TNTs), after anodic oxidation and grafted with PDA (TNTs/PDA) and final condition after silver incorporation (TNTs/PDA/Ag).

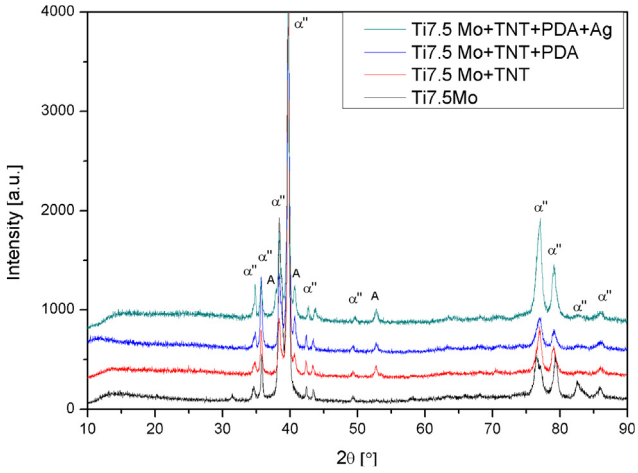

Fig. 3. X-ray diffraction pattern of the surfaces: substrate (Ti7.5Mo alloy); TNTs; TNTs/PDA and TNTs/PDA/Ag.

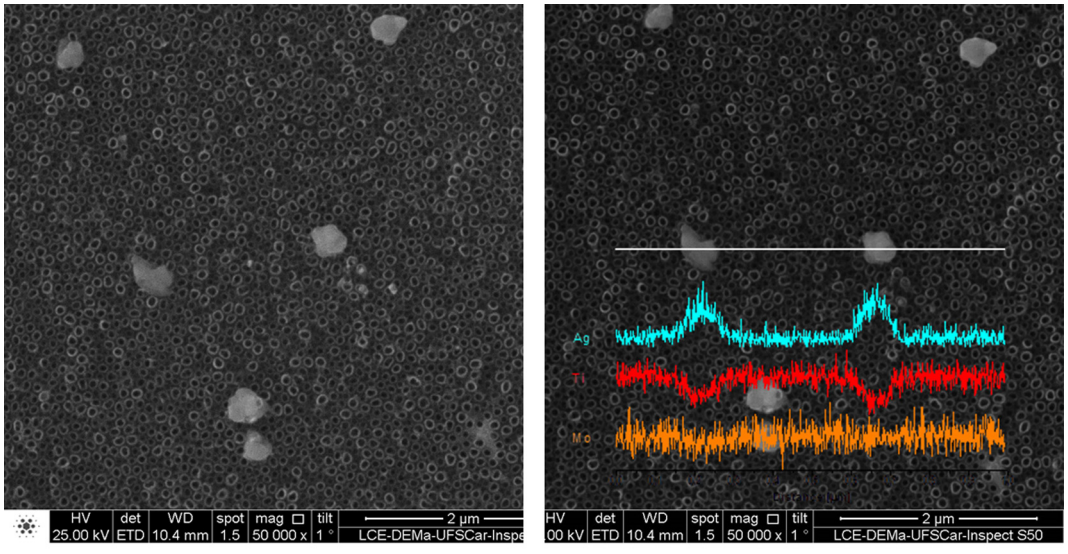

Fig. 2. (a) Top view SEM images of the Ti7.5Mo alloy surface after PDA grafted and immersion in $AgNO_3$ and (b) EDS showing silver nanoparticles.

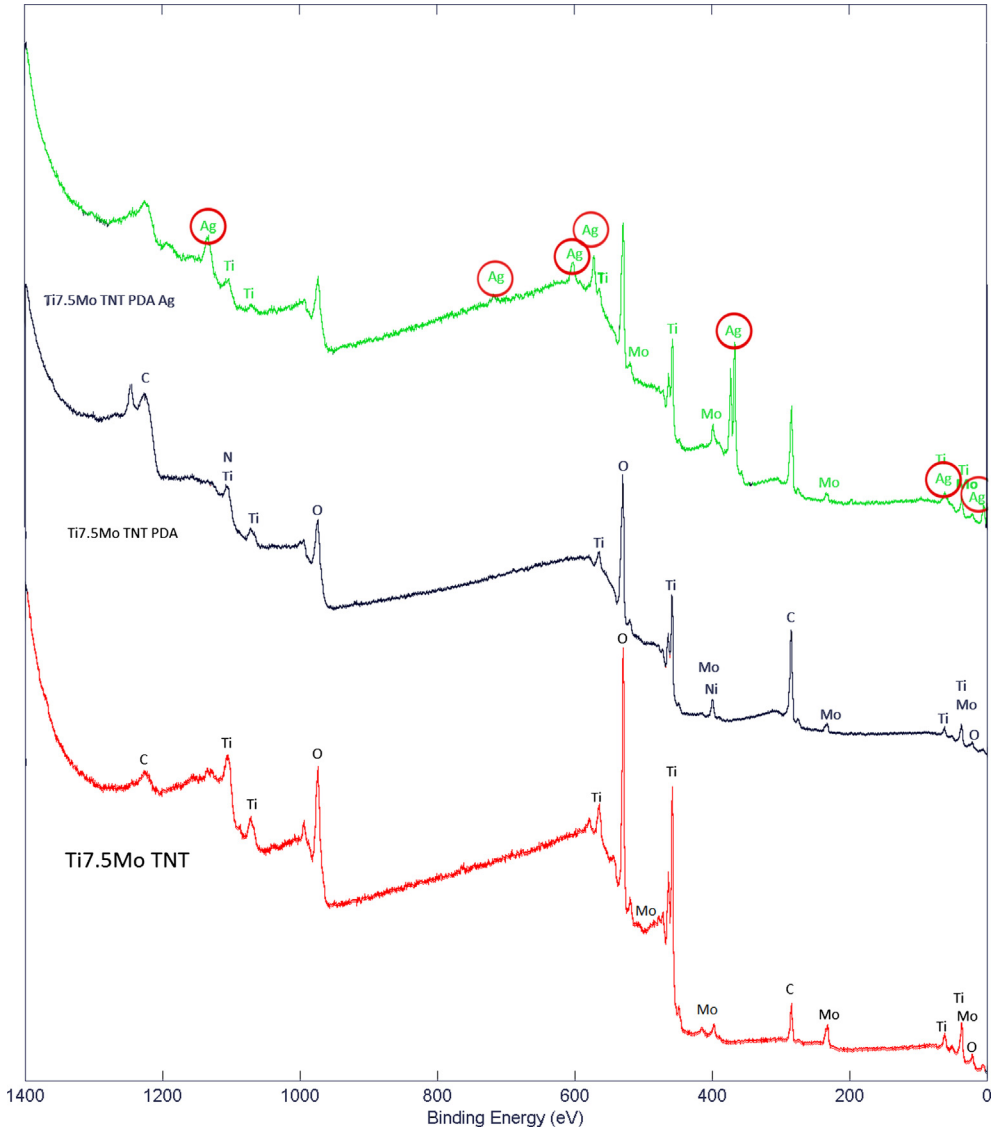

Fig. 4. XPS spectra of the TNTs, TNTs/PDA and TNTs/PDA/Ag.

Table 1
Atomic percentage of the elements for each group.

Sample	Elements – Atomic percentage (%)					
	O	Ti	C	N	Mo	Ag
TNT	48.8	22.7	21.6	5.3	1.5	< 0.1
PDA	49.00	22.70	21.83	5.00	1.43	< 0.1
PDA/Ag	32.60	9.67	46.80	7.07	0.53	3.33

The presence of silver was confirmed by the peaks as shown in the figure. The associated data related to the atoms present, and the position and atomic concentration in the samples are shown in Table 1. The presence of the molybdenum and titanium after PDA coating leading us to concluded that the layer thickness is very thin.

The surface properties such as topography (roughness), chemistry and wettability will influence the answer of the biomaterial after its insertion in biological environment. Studies have been demonstrated that surface topography affects directly the wettability and the corresponding biological response. The wettability behavior should be evaluated in macroscale, microscale or nanoscale levels. For example, in microscopic level, a substantial increase of the differentiation and maturation of osteoblast cells on micro-rough surface, compare to smooth surface have been verified. In macroscopic level, fibrous capsule formation or osseointegration with low bone/implant contact have been attributed to smooth surfaces while the enhance of osseointegration and higher levels of bone/implant contact have been associated to rough surface [25]. In addition, surface chemistry also affects the surface energy because affects the charge of the surface. Generally, the average wettability of a surface is evaluated by using static contact angle measurements. The sessile drop method is the probably the most used technique for measuring the contact angle of a liquid on a surface. A liquid drop of a known volume is dropped on the surface and a camera capture the boundary of the drop.

In our study, this technique was used to evaluate the influence of PDA/Ag coating on the wettability. The contact angle (CA) for surfaces containing TiO_2 nanotubes was found to be 8.99° which increased to 14.37° after PDA/Ag coating. In both cases, the surfaces were hydrophilic found the contact angle < 90°. The proximity between the values confirmed that PDA does not significantly alters the surface wettability. Surfaces containing nanotubes exhibited lower contact angle values and have high wettability. However, when coated with only PDA exhibited slightly higher contact angle [10].

Table 2
Means values (CFU log10) and p values obtained for the biofilm.

Group	Microbial biofilms CFU log10			
	C. albicans	p Value	*S. aureus*	p Value
TNT	5.620	0.0002	8.110	0.0048
TNT/PDA/Ag	0.000	0.000	0.000	0.000

3.2. In vitro studies

3.2.1. Bacterial adhesion

The surfaces were evaluated in vitro by incubated the samples with *Candida albicans* and *Streptococcus aureus* (two species biofilms) for 48 h. Mean and standard deviation values of the CFU/ml (log10) obtained in the experimental conditions tested for each biofilms group are shown in Table 2.

The results clearly confirmed TNTs/PDA/Ag samples exhibited strong antibacterial activity. For the group containing TiO_2 nanotubes the presence of colonies of C. *albicans* and S. *aureus* is observed, while samples with antibacterial coating (Ti7.5Mo + TNT + PDA + Ag samples) killed bacteria. It has been observed that samples with PDA/Ag exerted a satisfactory effect for C. *albicans* and S. *aureus*, avoiding biofilms formation. The silver antibacterial action mechanism can occur by release of silver ions or by direct contact of silver with bacteria. The bacterial death of the samples covered with PDA/Ag can be explained due to the electrostatic interaction between of the silver positive charge and the bacterial membrane negative charge, thus increasing the permeability of the membrane with diffusion of silver ions in the cells and migration of the matrix intracellularly out of the cell, causing cell decline and death [26]. When the silver ions release occurs, they move inside the cell and attack several sites leading to the inactivation of critical physiological functions that can break the cell wall, cause protein denaturation, block cellular respiration and finally cause microbial death [27]. According to Li et al. [28] when bacterial death occurs by direct contact with silver, the potential for lethality is even greater. According to Agnihotri et al.[29], the bactericidal action mechanism of silver can occur by: direct contact with immobilized silver nanoparticles, contact with silver nanoparticles released from a colloidal solution, or ion-mediated of silver released from immobilized silver nanoparticles. However, in their studies, the best disinfection results were obtained by direct contact with immobilized silver nanoparticles, far beyond the substrates that liberated silver only in its ionic form.

3.2.2. Cell adhesion

The cytotoxicity was evaluated with lactate dehydrogenase (LDH) release assay in medium of ADSCs cells after 24 h of culture. The coating PDA/Ag no affect LDH specific activity and no significance between groups was registered (Fig. 5), in other words, PDA/silver coating is not cytotoxic.

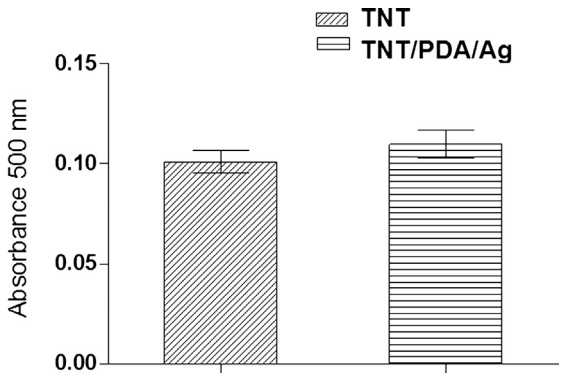

Fig. 5. Cytotoxicity of different surfaces measured using LDH assay, data represented as absorbance which is proportional to LDH released by the cells indicating the cytoxicity.

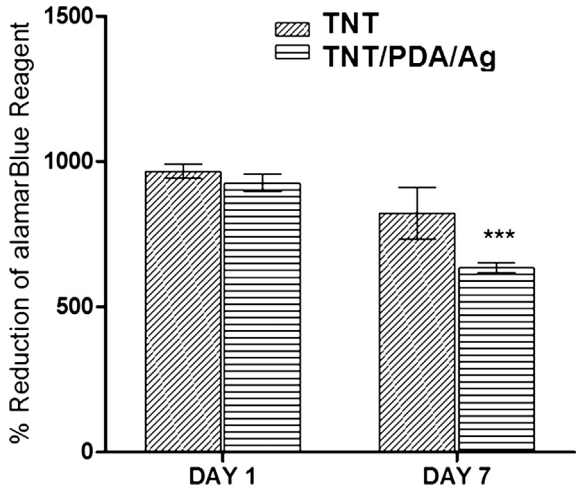

Fig. 6. Percentage reduction of Alamar blue indicating proliferation of ADSCs on different surfaces.

The viability cells were characterized using CellTiter-Blue® assay, in which the viable cells are able of reduce the Resazurin to Resorufin. Therefore, there is a direct correlation between the reduction of CellTiter-Blue® reagent in the growth media and the quantity/proliferation of living cells. Fig. 6 shows that cell proliferation on the TNT did not show remarkable differences in cellular activity from Day 1 to Day 7 ($p > 0.05$ for two groups) while cells activity reduced abruptly on TNT/PDA/Ag from Day 1 to Day 7. This may be due to the fact that the silver is known to be toxic to the cells.

Cell adhesion and proliferation were evaluated by staining the cells with Rhodamine-phalloidin and DAPI after 1 and 7 days of culture. Rhodamine-phalloidin has affinity with a red-orange fluorescent dye, tetramethyl rhodamine (TRITC) and stain cell actin filaments. This way is possible to analyze the coverage of actin filaments on the surfaces, on different days. Also, rhodamine-phalloidin provides analysis of elongation of cytoskeleton. DAPI binds DNA adenine-thymine regions, thus, is possible quantify the number of nuclei (cells) that are present on a surface. Fig. 7 shows the fluorescence microscopy analysis of ADSCs cultured at 1 and 7 days on TNT and TNT/PDA/Ag. The results indicate that all the surfaces promoted cell growth from day 1 to day 7 for TNT whereas for TNT/PDA/Ag similar number of cells were observed. This may be due to the fact that silver is known to be toxic to cells. However, there are still cells present on TNT/PDA/Ag which are alive, and number of cells after 7 days is similar to that of after 1 day. The results indicate that the cells are adhering but not proliferating on TNT/PDA/Ag.

The morphology of ADSCs on TNT and TNT/PDA/Ag surfaces was investigated using SEM after 7 days of culture. Fig. 8 shows the cell membrane and the filopodia of the ADSCs that anchored in the nanotubes. Several studies have shown that the presence of nanostructures is able to stimulate adhesion and cytoskeletal organization of osteoblasts, however, studies that evaluate cellular behavior on surface with silver indicate less spreading and less filopodia.

3.3. In vivo studies – Zebrafish animal model

3.3.1. Evaluation of locomotor activity

The results showed that the treatment with TiO_2 nanotubes (TNT) and TiO_2 nanotubes/PDA/Ag after immersion at time Day 1 (1D), Day 4 (4D) and Day 7(7D) did not cause altered locomotor activity between groups in the behavioral assay at 5 dpf and 7 dpf ($p \geq 0.05$) (Figs. 9 and

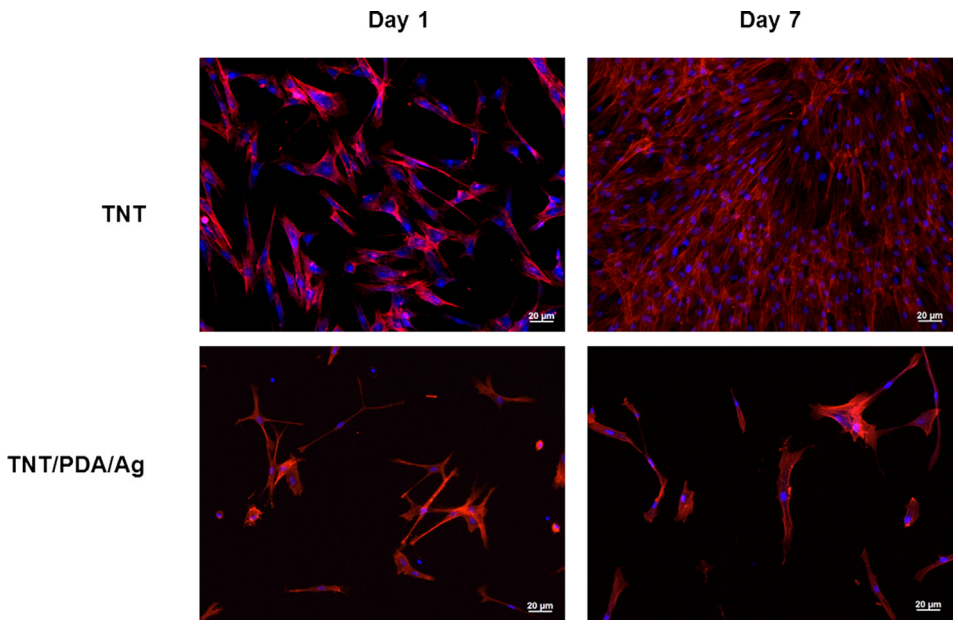

Fig. 7. Fluorescence microscopy images of ADSCs on different surfaces after 1 and 7 days of culture.

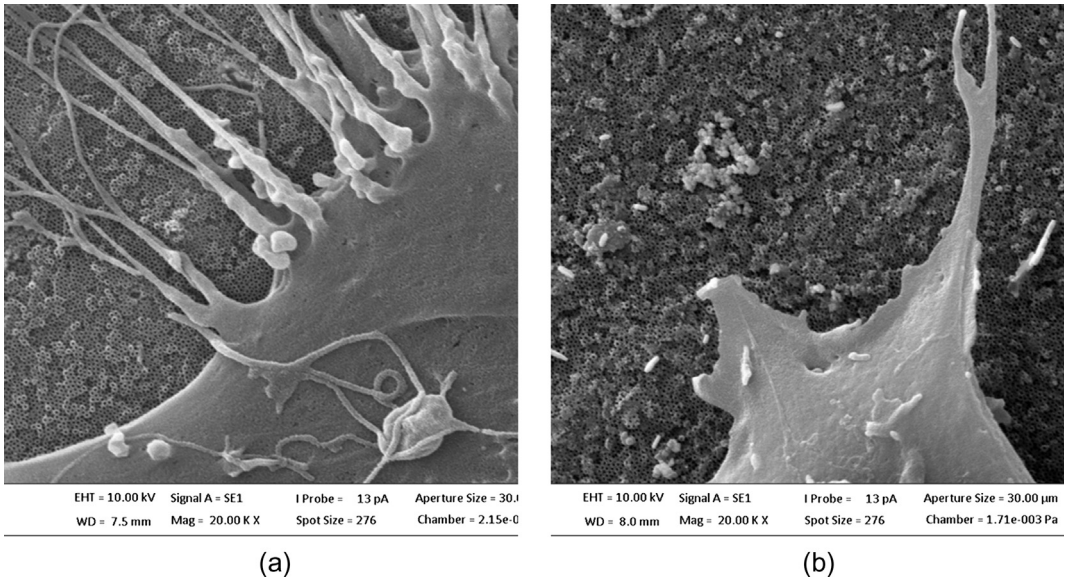

Fig. 8. Scanning Electron Microscopy images of cells on different surfaces.

10). For distance travelled at 5 dpf, the mean ± SEM of the TNT (n = 15), 1D (n = 15), 4D (n = 15), 7D (n = 14), and Control (n = 15) groups were, respectively: 3.56 ± 0.06; 3.39 ± 0.10; 3.65 ± 0.03; 3.41 ± 0.09 and 3.60 ± 0.05 (Fig. 9a). For velocity at 5 dpf, the mean ± SEM of the TNT, 1D, 4D, 7D and Control groups were, respectively: 0.13 ± 0.06; −0.03 ± 0.10; 0.22 ± 0.03; −0.01 ± 0.09 and 0.17 ± 0.05 (Fig. 9b). At 7 dpf, the mean ± SEM for distance travelled of the TNT (n = 15), 1D (n = 15), 4D (n = 14), 7D (n = 14), and Control (n = 15) groups were, respectively: 3.66 ± 0.08; 3.62 ± 0.03; 3.33 ± 0.22; 3.72 ± 0.08 and 3.67 ± 0.04. For velocity at 7dpf, the mean ± SEM of the TNT, 1D, 4D, 7D and Control groups were, respectively: 0.23 ± 0.04; 0.19 ± 0.03; 0.13 ± 0.06; 0.29 ± 0.08 and 0.024 ± 0.04.

According literature [17,30,31], silver has the potential to alter the neurodevelopment and cause behavioral retardation. Its toxicity depends directly of the concentration and in some causes it very high can be hyperactivity of embryo. In our study, silver particles were not detected in solution using voltammetry technique and these results are in line with our zebrafish analyses, once the silver presence on the solution could affect the activity.

4. Conclusions

Silver was incorporated on the Ti7.5Mo alloy surface containing TiO2 nanotubes using polydopamine assisted immobilization technique. The surfaces exhibited antibacterial behavior and although most of studies associated the bacteria killed to silver release, in our study, bacteria died due to contact with surface. However, the presence of silver on the surfaces inhibited the cell proliferation. In vivo studies with zebrafish confirmed that no silver in solutions once the behavior of embryos was not changed. Results showed the treatment can be used but studies considering long term analysis need to do.

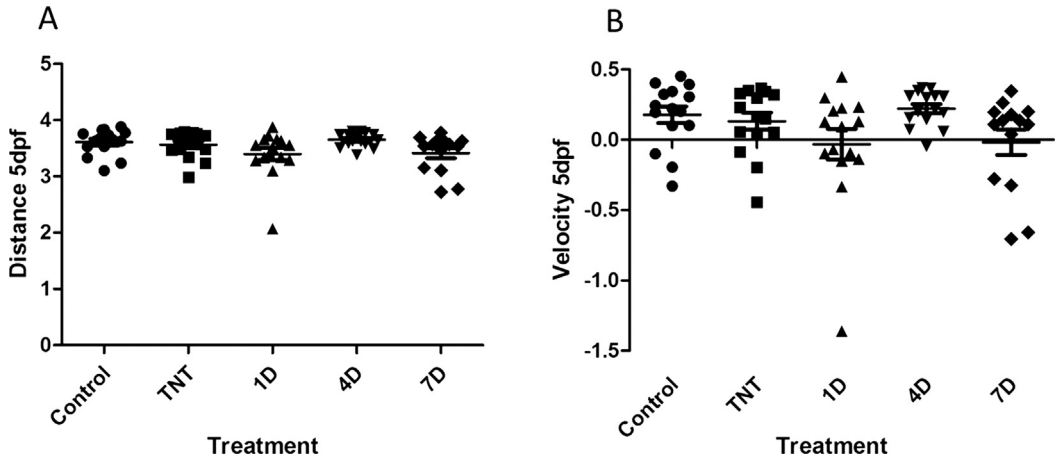

Fig. 9. Effect of the TiO_2 nanotubes and TiO_2 nanotubes/PDA/Ag on locomotor activity response in zebrafish at 5 days post-fertilization. (A) Distance travelled and (B) Velocity.

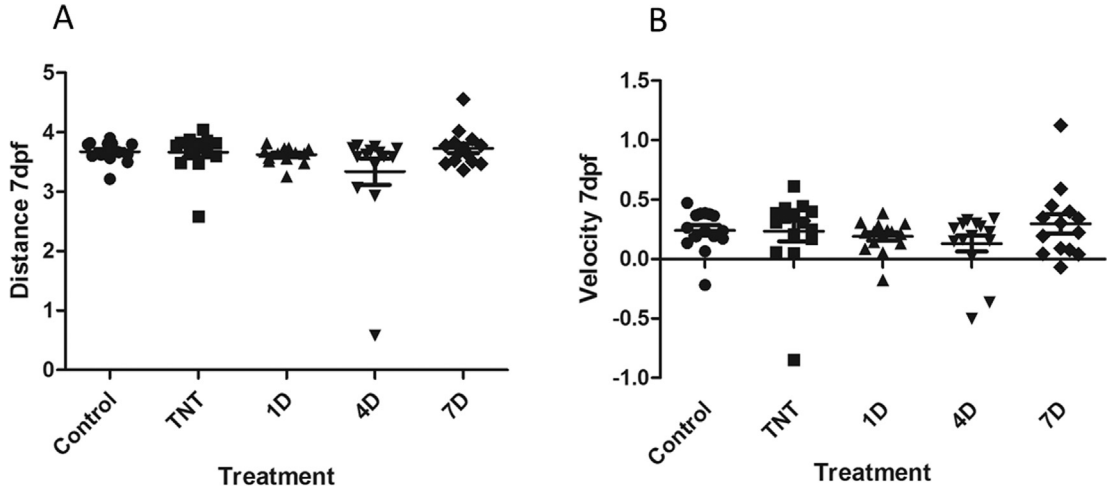

Fig. 10. Effect of the TiO_2 nanotubes and TiO_2 nanotubes/PDA/Ag on locomotor activity response in zebrafish at 7 days post-fertilization (dpf). (A) Distance travelled and (B) Velocity.

Acknowledgments

This research was supported by CNPq – National Council for Scientific and Technological Development (486352-2013-7 and 309469/2015-5), CAPES – Coordination for the Improvement of Higher Level – or Education – Personnel (99999.006563/2014-7), FAPESP – São Paulo Research Foundation (2014/15640-8 and 2013/08200-9). This work was partially supported by Natural Science and Engineering Research Council of Canada and the Canada Research Chair in Biomaterials and Bioengineering for the Innovation in Surgery.

References

[1] S. Minagar, J. Wang, C.C. Berndt, E.P. Ivanova, C. Wen, Cell response of anodized nanotubes on titanium and titanium alloys, J. Biomed. Mater. Res. – Part A (2013), http://dx.doi.org/10.1002/jbm.a.34575.

[2] S. Minagar, C.C. Berndt, T. Gengenbach, C. Wen, Fabrication and characterization of TiO_2–ZrO_2–$ZrTiO_4$ nanotubes on TiZr alloy manufactured via anodization, J. Mater. Chem. (2014), http://dx.doi.org/10.1039/c3tb21204a.

[3] T.K. Monsees, K. Barth, S. Tippelt, K. Heidel, A. Gorbunov, W. Pompe, R.H.W. Funk, Effects of different titanium alloys and nanosize surface patterning on adhesion, differentiation, and orientation of osteoblast-like cells, Cells Tissues Org. (2005), http://dx.doi.org/10.1159/000086749.

[4] P. Capellato, B.S. Smith, K.C. Popat, A.P.R. Alves Claro, Cellular functionality on nanotubes of Ti-30Ta alloy, Mater. Sci. Forum (2015), http://dx.doi.org/10.4028/www.scientific.net/MSF.805.61.

[5] J. Hasan, R.J. Crawford, E.P. Ivanova, Antibacterial surfaces: the quest for a new generation of biomaterials, Trends Biotechnol. (2013).

[6] C.R. Arciola, D. Campoccia, P. Speziale, L. Montanaro, J.W. Costerton, Biofilm formation in Staphylococcus implant infections. A review of molecular mechanisms and implications for biofilm-resistant materials, Biomaterials (2012), http://dx.doi.org/10.1016/j.biomaterials.2012.05.031.

[7] H. Li, Q. Cui, B. Feng, J. Wang, X. Lu, J. Weng, Antibacterial activity of TiO_2 nanotubes: influence of crystal phase, morphology and Ag deposition, Appl. Surf. Sci. (2013), http://dx.doi.org/10.1016/j.apsusc.2013.07.076.

[8] L. Zhao, H. Wang, K. Huo, L. Cui, W. Zhang, H. Ni, Y. Zhang, Z. Wu, P.K. Chu, Antibacterial nano-structured titania coating incorporated with silver nanoparticles, Biomaterials (2011), http://dx.doi.org/10.1016/j.biomaterials.2011.04.040.

[9] S.-H. Uhm, S.-B. Lee, D.-H. Song, J.-S. Kwon, J.-G. Han, K.-N. Kim, Fabrication of bioactive, antibacterial TiO_2 nanotube surfaces, coated with magnetron sputtered Ag nanostructures for dental applications, J. Nanosci. Nanotechnol. 14 (2014) 7847–7854, http://dx.doi.org/10.1166/jnn.2014.9412.

[10] S. Zhong, R. Luo, X. Wang, L. Tang, J. Wu, J. Wang, R. Huang, H. Sun, N. Huang, Effects of polydopamine functionalized titanium dioxide nanotubes on endothelial cell and smooth muscle cell, Colloid Surf. B Biointerfaces (2014), http://dx.doi.org/10.1016/j.colsurfb.2014.01.030.

[11] S. Saidin, P. Chevallier, M.R. Abdul Kadir, H. Hermawan, D. Mantovani, Polydopamine as an intermediate layer for silver and hydroxyapatite immobilisation on metallic biomaterials surface, Mater. Sci. Eng. C (2013), http://dx.doi.org/10.1016/j.msec.2013.07.026.

[12] Z. Jia, P. Xiu, M. Li, X. Xu, Y. Shi, Y. Cheng, S. Wei, Y. Zheng, T. Xi, H. Cai, Z. Liu, Bioinspired anchoring AgNPs onto micro-nanoporous TiO_2 orthopedic coatings: Trap-killing of bacteria, surface-regulated osteoblast functions and host responses, Biomaterials (2016), http://dx.doi.org/10.1016/j.biomaterials.2015.10.035.

[13] A.L.A. Escada, R.Z. Nakazato, A.P.R.A. Claro, Growth of TiO_2 nanotubes by anodization of Ti–7.5Mo in NH_4F solutions, Nanosci. Nanotechnol. Lett. (2013), http://dx.doi.org/10.1166/nnl.2013.1557.

[14] A.L.A. Escada, J.P.B. Machado, R.Z. Nakazato, A.P.R. Alves Claro, Growth of calcium phosphate coating on Ti-7.5Mo alloy after anodic oxidation, Defect Diffus.

Forum (2013), http://dx.doi.org/10.4028/www.scientific.net/DDF.334-335.297.
[15] J.M. Chaves, A.L.A. Escada, A.D. Rodrigues, A.P.R. Alves Claro, Characterization of the structure, thermal stability and wettability of the TiO_2 nanotubes growth on the Ti-7.5Mo alloy surface, Appl. Surf. Sci. (2016), http://dx.doi.org/10.1016/j.apsusc.2016.02.017.
[16] N.F. Belyaeva, V.N. Kashirtseva, N.V. Medvedeva, Y. Khudoklinova, O.M. Ipatova, A.I. Archakov, Zebrafish as a model system for biomedical studies, Biochem. Suppl. Ser. B: Biomed. Chem. 3 (2009) 343–350.
[17] C. Chakraborty, A.R. Sharma, G. Sharma, S. Lee, Zebrafish: A complete animal model to enumerate the nanoparticle toxicity, J. Nanobiotechnol. 14 (2016), http://dx.doi.org/10.1186/s12951-016-0217-6.
[18] M.F. Brugnera, M. Miyata, C.Q. Fujimura Leite, M.V.B. Zanoni, Silver ion release from electrodes of nanotubes of TiO_2 impregnated with Ag nanoparticles applied in photoelectrocatalytic disinfection, J. Photochem. Photobiol. A Chem. (2014), http://dx.doi.org/10.1016/j.jphotochem.2013.12.020.
[19] C. Radheshkumar, H. Münstedt, Antimicrobial polymers from polypropylene/silver composites-Ag+ release measured by anode stripping voltammetry, React. Funct. Polym. (2006), http://dx.doi.org/10.1016/j.reactfunctpolym.2005.11.005.
[20] A.I. Kamenev, K.A. Lushov, Determination of silver by stripping voltammetry at composite pyrocarbon-glass ceramic electrodes, J. Anal. Chem. 56 (4) (2001) 380–383.
[21] A.L.A. Escada, J.P.B. Machado, R.Z. Nakazato, A.P.R. Alves Claro, Obtaining of nanoapatite in Ti-7.5Mo surface after nanotube growth, Mater. Sci. Forum (2012), http://dx.doi.org/10.4028/www.scientific.net/MSF.727-728.1199.
[22] P. Van Viet, N.C. Trung, P.M. Nhut, L. Van Hieu, C.M. Thi, The fabrication of the antibacterial paste based on TiO_2 nanotubes and Ag nanoparticles-loaded TiO_2 nanotubes powders, J. Exp. Nanosci. (2017), http://dx.doi.org/10.1080/17458080.2017.1301685.
[23] C. Wu, G. Zhang, T. Xia, Z. Li, K. Zhao, Z. Deng, D. Guo, B. Peng, Bioinspired synthesis of polydopamine/Ag nanocomposite particles with antibacterial activities, Mater. Sci. Eng. C (2015), http://dx.doi.org/10.1016/j.msec.2015.05.032.
[24] L. Zhao, P.K. Chu, Y. Zhang, Z. Wu, Antibacterial coatings on titanium implants, J. Biomed. Mater. Res. – Part B Appl. Biomater. (2009), http://dx.doi.org/10.1002/jbm.b.31463.
[25] R.A. Gittens, R. Olivares-Navarrete, Z. Schwartz, B.D. Boyan, Implant osseointegration and the role of microroughness and nanostructures: lessons for spine implants, Acta Biomater. (2014), http://dx.doi.org/10.1016/j.actbio.2014.03.037.
[26] J.S. Kim, E. Kuk, K.N. Yu, J.H. Kim, S.J. Park, H.J. Lee, S.H. Kim, Y.K. Park, Y.H. Park, C.Y. Hwang, Y.K. Kim, Y.S. Lee, D.H. Jeong, M.H. Cho, Antimicrobial effects of silver nanoparticles, Nanomed. Nanotechnol. Biol. Med. (2007), http://dx.doi.org/10.1016/j.nano.2006.12.001.
[27] M.Y. Lan, C.P. Liu, H.H. Huang, S.W. Lee, Both enhanced biocompatibility and antibacterial activity in Ag-decorated TiO_2 nanotubes, PLoS One (2013), http://dx.doi.org/10.1371/journal.pone.0075364.
[28] Y. Li, W.K. Leung, K.L. Yeung, P.S. Lau, J.K.C. Kwan, A multilevel antimicrobial coating based on polymer-encapsulated ClO_2, Langmuir (2009), http://dx.doi.org/10.1021/la901974d.
[29] S. Agnihotri, S. Mukherji, S. Mukherji, Immobilized silver nanoparticles enhance contact killing and show highest efficacy: elucidation of the mechanism of bactericidal action of silver, Nanoscale (2013), http://dx.doi.org/10.1039/c3nr00024a.
[30] C.M. Powers, T.A. Slotkin, F.J. Seidler, A.R. Badireddy, S. Padilla, Silver nanoparticles alter zebrafish development and larval behavior: distinct roles for particle size, coating and composition, Neurotoxicol. Teratol. (2011), http://dx.doi.org/10.1016/j.ntt.2011.02.002.
[31] G. Ašmonaite,, S. Boyer, K.B. de Souza, B. Wassmur, J. Sturve, Behavioural toxicity assessment of silver ions and nanoparticles on zebrafish using a locomotion profiling approach, Aquat. Toxicol. (2016), http://dx.doi.org/10.1016/j.aquatox.2016.01.013.